Simple three-state lattice model for liquid water

Alina Ciach,[1] Wojciech Góźdź,[1] and Aurélien Perera[2]
[1]*Institute of Physical Chemistry, Polish Academy of Sciences, Kasprzaka 44/52, 01-224 Warsaw, Poland*
[2]*Laboratoire de Physique Théorique de la Matiére Condensée (UMR CNRS 7600), Université Pierre et Marie Curie, 4 Place Jussieu, F75252, Paris cedex 05, France*
(Received 18 April 2008; published 19 August 2008)

A simple three-state lattice model that incorporates two states for locally ordered and disordered forms of liquid water in addition to empty cells is introduced. The model is isomorphic to the Blume-Emery-Griffith model. The locally ordered (O) and disordered (D) forms of water are treated as two components, and we assume that the density of the D component is larger. The density of the sample is determined by the fraction of cells occupied by the O and D forms of water. Due to the larger density of the D state, the strength of the van der Waals (vdW) interactions increases in the direction O-$O<O$-$D<D$-D. On the other hand, the H-bond interactions are assumed only for the O-O pairs. For the vdW and H-bond interaction parameters and the density ratio of the close-packed and ice forms of water compatible with experimentally known values, we find liquid-vapor and liquid-liquid transitions and the corresponding critical points in good agreement with other approaches. Water anomalies are correctly predicted within the mean-field approximation on a qualitative level.

DOI: 10.1103/PhysRevE.78.021203 PACS number(s): 61.20.Gy

I. INTRODUCTION

Interactions among water molecules are characterized by the existence of the hydrogen bond, which is a strongly directional interaction. Combination of the directionality and the geometry of the water molecule gives rise to pronounced local tetrahedral ordering of the molecules in the liquid phase. The competition between the strong local order and the global disorder inherent to the liquid state is at the origin of the several anomalous properties of water, such as the maximum of density at 4C. The idea that such a competition could give rise to the coexistence of two types of water domains—a low-density ordered one and a high-density disordered one—dates back to Roentgen [1] in 1892 and has known several rebirths since then, notably by Pauling [2] and later by Frank and Wen [3] and Robinson *et al.* [4]. However, spectroscopic experiments [5] and computer simulations [6] confirm only indirectly the fact that water would be formed of a coexistence of such two types of domains of water molecules, and most probably in supercooled states. Nevertheless, the two-state models for water have been very much appealing in providing a simple physical picture of its structure and in explaining its anomalies. There are other indirect indications that water can be in two different local states, such as, for example, in aqueous mixtures. There are several experimental pieces of evidence that water in the first solvation shell near ions is in a quite different state than in the bulk [7], which leads to marked differences in the viscosity of these aqueous ionic solutions. Similarly, the aqueous solvation of small polar and nonpolar molecules is often discussed [8] in terms of kosmotropy versus chaotropy, depending on their ability to increase or decrease the local order of water, which is also in relation to the so-called hydrophobic effect [9]. Water near amino acids has been found to have a different structural ordering by neutron-scattering experiments [10]. Temperature- and pressure-induced structural isosbestic points in neat water [11] provide additional experimental support for a two-state description of liquid water.

The implicit existence of the coexistence of two types of liquid states in water implies possibility of the existence of a second critical point, presumably in the supercooled region [12–14]. The existence of such a critical point has been at the heart of much debates [12–17] and has motivated the appearance of two-state models, both lattice and off-lattice, such as in Refs. [13,16,18]. It is worth mentioning that recent critical-point-free approaches are also able to describe the anomalies of cold water [19,20].

Lattice models for water have a long history, dating back to the early work of Bell in 1972 [21]. A detailed list of such models is given in Ref. [13]. In these early models, water is often treated with full tetrahedral orientational dependence more or less explicitly described. The main emphasis of such models is to capture the fact that the H bonds would form a network. Recent studies [22–24] of the core-softened off-lattice models [25] indicate that spherically symmetric interactions are equally able to capture the waterlike anomalies at low enough temperatures. These results suggest that the water anomalies should not need an explicit description of the details of the interactions even at microscopical level.

The lattice- and continuum-space models introduced in Refs. [13,14,16,18,26] are quite successful in predicting the thermodynamics and structure of water, but usually they are rather complex. For example, in Ref. [16] orientational degrees of freedom of water molecules that occupy a bcc lattice are taken into account. Apart from the van der Waals interaction between the occupied nearest-neighbor (NN) sites, the H-bond energy contribution is assumed for properly oriented NNs. The open network is promoted by an energy penalty for occupied sites around the H-bonded pair of sites. The advantage of this model is a possibility of predicting stability of fluid and solid phases. Unfortunately, on the simple mean-field (MF) level the model predicts no liquid-liquid separation, which is found beyond the MF, however. Fundamental cells with 98 states (and 98 energies) are considered in order to obtain the equation of state and phase diagram in Ref. [16]. The complexity of the model and the failure of the simple MF makes the extension of the model to aqueous

mixtures rather difficult. In Refs. [27,28] extensions of the simpler, off-lattice mean-field model of water [29] have been proposed to mixtures with *nonpolar* molecules [27,28]. However, we are interested in mixtures of water with *polar* molecules (alcohols, amides, and other weak amphiphiles), because such mixtures show intriguing properties [30]; to some extent they resemble microemulsions formed in binary water-surfactant and ternary oil-water-surfactant mixtures. Universal properties of binary water-surfactant and ternary oil-water-surfactant mixtures are described by simple generic lattice models [31–35] where water is treated as an ordinary liquid, because the effective energies involved in the self-assembly are higher than the energy involved in local ordering of water. Self-assembly of weak amphiphiles such as alcohols may compete with local ordering of water, and in the case of weak amphiphiles standard models of microemulsions are oversimplified. To understand the origin of their peculiarities it is desirable to introduce a simple model, yet capable of reproducing the special properties of pure water. To this end we need a simple model for water in the first place.

Our purpose here is a construction of a generic lattice model which correctly predicts the qualitative properties of water and is as simple as possible. In general, the generic model represents the simplest system belonging to the class of systems exhibiting the same universal properties. The universal properties result from collective phenomena, where fluctuations over large length scale play the dominant role. The details of the local molecular structure are irrelevant, because these local details are averaged over large volume. The famous example of universal properties are the same values of the critical exponents for the gas-liquid critical point in simple fluids, Curie point in magnets, and demixing critical points in alloys. In the case of simple fluids such a generic model for the gas-liquid separation is the lattice-gas model, isomorphic to the Ising model for magnets. The physics of the gas-liquid critical point of water is also correctly predicted by the standard lattice-gas model. At high densities and low temperatures, however, the standard lattice-gas model is oversimplified. Here we introduce a very simple, three-state lattice model capable of predicting the special features of water. The model turns out to be of the same form as the Blume-Emery-Griffith (BEG) model [36].

II. CONSTRUCTION OF THE GENERIC MODEL

In the lattice-gas models one divides space into cubic cells of a size comparable to the size of molecules. The microscopic state of the system is determined by specifying the state of each cell, instead of describing the states of all molecules. In the simplest lattice-gas model, isomorphic to the Ising model, just two states of each cell are distinguished: the cell can be either occupied or unoccupied by the center of mass of the molecule. In liquid water some molecules form H bonds with their neighbors. The H bonds are associated with formation of the local tetrahedral structure and with larger volume per molecule than in the disordered state. The density of the whole sample is thus determined by the fraction of molecules that form the local tetrahedral structure. It is necessary to distinguish between the locally ordered and locally disordered states, and postulate proper probability measures for each spatial distribution of these states, to be able to predict the density of the sample for given intensive parameters.

The distinction between the presence and absence of the local tetrahedral order is necessary for reproducing the special properties of water. The question is if additional information about the structure is necessary for predicting the water anomalies. We shall assume that the necessary and sufficient information about the state of the sample is given when one specifies which cells are empty and selects from the remaining cells those with the tetrahedral order. Such partial information about the state of the sample is called the mesoscopic state. Our hypothesis is that for a description of collective phenomena leading to the density anomaly, no additional information about the local order is necessary, provided that the energetics of the system is properly taken into account in the probability measure $\propto \exp(-\beta H)$. Here $\beta = 1/kT$, with k and T the Boltzmann constant and temperature, respectively, and $H=E-\mu N$ is the mesoscopic Hamiltonian—a function that relates energy minus chemical potential times the number of particles to each mesoscopic state. H is derived below. The above hypothesis will be verified by comparing the predictions of the mesoscopic model with experiments.

We should stress that in the mesoscopic description we lose the information about the number of microscopic states in the cells occupied by the locally ordered and locally disordered water. It is expected that the entropy associated with local ordering in the cell occupied by the locally ordered water is lower than the entropy associated with local ordering in the cell occupied by the locally disordered water. In the mesoscopic model this difference in entropy associated with *local* ordering is disregarded. The results obtained in the mesoscopic model should shed light on the role of the entropy of the *local* ordering for the water anomalies.

The locally disordered and locally ordered states will be labeled 1 and 2, respectively, and the state representing the empty cell will be labeled 3. In order to introduce the Hamiltonian, we should first choose the proper size of the unit cell. For fixed volume the ratio between the number of molecules in the closely packed case (no H bonds) and in the perfect tetrahedral structure is

$$\frac{\rho_{HDW}}{\rho_{LDW}} = 1 + 2\delta, \tag{1}$$

where ρ_{HDW} and ρ_{LDW} denote the densities in the close-packed and perfect tetrahedral structure, respectively, and δ is the model parameter defined by the above equation.

Let us assume for a moment that only empty cells and state 2 are allowed. The natural choice for the volume v of the lattice cell is the volume per molecule in the perfect tetrahedral structure, v_0. With this choice the whole density interval $(0, \rho_{LDW})$ can be obtained from the model where the cells can be either unoccupied or occupied by just one molecule. The density ρ_{LDW} corresponds to the occupancy of all cells. Let us now assume that only empty cells and state 1 are allowed. In the model where the cells can be either unoccu-

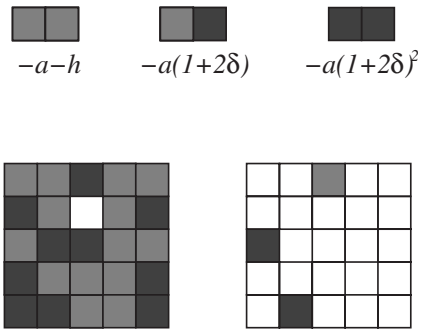

FIG. 1. Nonvanishing nearest-neighbor interactions (upper panel) and two-dimensional cross sections through a part of a system in two mesoscopic states (lower panel). a and h represent the van der Waals and H-bond energy parameters, respectively, and 2δ is the relative difference between the close-packed and ice densities (1). Dark-gray and light-gray squares represent cross sections through cells occupied by the closely packed and by the open tetrahedral structures, respectively, and the open squares represent empty cells. The mesoscopic state shown in the lower-left panel is typical in the (supercritical) liquid, and the mesoscopic state shown in the lower-right panel is typical for vapor. Probability that a given mesoscopic state appears is proportional to the Boltzmann factor $\exp[-\beta(E-\mu N)]$, where the energy E is given by the sum of energies of all NN pairs (according to the upper panel) and the number of molecules is $N=N_1(1+2\delta)+N_2$, with N_1 and N_2 denoting the number of dark-gray and light-gray cells, respectively [see (9) and (2)].

pied or occupied by just one molecule, the cell-volume should be $v=v_0\rho_{LDW}/\rho_{HDW}<v_0$, so that the occupancy of all cells corresponds to the density ρ_{HDW}. If both states and empty cells are possible, we should be able to relate the density of the liquid to the fraction of the cells in state 1 and the fraction of the cells in state 2. We choose the volume of the unit cell equal to the volume per molecule in the perfect tetrahedral structure, v_0, and assume that there is one molecule per cell in state 2, whereas the cell in state 1 contains ρ_{HDW}/ρ_{LDW} molecules.

The energy of the system depends on the number of H-bonded pairs and on the van der Waals (vdW) interaction. We shall assume that only NNs interact. This assumption was verified for the vdW interaction in the context of the gas-liquid transition in the lattice-gas models in a large number of works. Clearly, an NN interaction is consistent with the short range of the H bonds. Since the H bonds are associated with the formation of tetrahedral structure, we assume that each pair of NNs that are both in state 2 contributes $-h$ to the system energy. The pair of NNs yields no contribution to the system energy if at least one of the two cells is empty. The vdW energy of a pair of the nn cells is $-a$ when both cells are in state 2, $-a(1+2\delta)$ if one cell is in state 1 and the other one is in state 2, and $-a(1+2\delta)^2$ if both NN cells are in state 1. Here a is the vdW parameter. The above form of interaction energies directly follows from different densities in the two states, Eq. (1), and the dependence of the vdW energy on the product of densities in the considered regions. Finally, the number of molecules in the system is equal to the number of cells in state 2 plus ρ_{HDW}/ρ_{LDW} times the number of cells in state 1. The above assumptions define the generic (or minimal) model (see Fig. 1).

The mesoscopic Hamiltonian can be written in terms of the operators representing the state occupancy, which are $\hat{\rho}_i(\mathbf{x})=1,0$ when the cell $\mathbf{x}$ is or is not in the state i, respectively. For each cell $\mathbf{x}$ the occupancy operators satisfy the condition $\Sigma_{i=1}^{3}\hat{\rho}_i(\mathbf{x})=1$. The above condition guarantees that each cell is in just one state, either 1, 2, or 3. The Hamiltonian is defined by

$$\mathcal{H}=-\sum_{\mathbf{x}}\sum_{i=1}^{d}\{a(1+2\delta)^2\hat{\rho}_1(\mathbf{x})\hat{\rho}_1(\mathbf{x}+\mathbf{e}_i)+(a+h)\hat{\rho}_2(\mathbf{x})\hat{\rho}_2(\mathbf{x}+\mathbf{e}_i)+a(1+2\delta)[\hat{\rho}_1(\mathbf{x})\hat{\rho}_2(\mathbf{x}+\mathbf{e}_i)+\hat{\rho}_2(\mathbf{x})\hat{\rho}_1(\mathbf{x}+\mathbf{e}_i)]\}-\mu\sum_{\mathbf{x}}[\hat{\rho}_2(\mathbf{x})+(1+2\delta)\hat{\rho}_1(\mathbf{x})]. \quad (2)$$

The first sum runs over all lattice cells $\mathbf{x}$, d is the space dimension, and $\mathbf{e}_i$ denotes the unit lattice vector in direction i, where $1\leqslant i\leqslant d$. With such a form we avoid double counting of the pairs of cells.

It is convenient to introduce new variables—the local concentration and site occupancy—corresponding to two order-parameters (OPs),

$$\hat{s}=\hat{\rho}_1-\hat{\rho}_2,\quad \hat{s}=1,-1,0, \quad (3)$$

$$\hat{s}^2=\hat{\rho}_1+\hat{\rho}_2,\quad \hat{s}^2=1,0, \quad (4)$$

where for the high-density water (HDW), low-density water (LDW), and vacuum, $\hat{s}=1$, -1, and 0 and $\hat{s}^2=1$, 1, and 0, respectively. The Hamiltonian in the new variables takes the familiar BEG-model form [36]

$$\mathcal{H}=-\sum_{\mathbf{x}}\sum_{i}\{J^{ll}\hat{s}(\mathbf{x})\hat{s}(\mathbf{x}+\mathbf{e}_i)+4J^{gl}\hat{s}^2(\mathbf{x})\hat{s}^2(\mathbf{x}+\mathbf{e}_i)+Q[\hat{s}(\mathbf{x})\hat{s}^2(\mathbf{x}+\mathbf{e}_i)+\hat{s}^2(\mathbf{x})\hat{s}(\mathbf{x}+\mathbf{e}_i)]\}-\mu\delta\sum_{\mathbf{x}}\hat{s}(\mathbf{x})-\mu(1+\delta)\sum_{\mathbf{x}}\hat{s}^2(\mathbf{x}), \quad (5)$$

where

$$J^{ll}=a\delta^2+\frac{h}{4}, \quad (6)$$

$$4J^{gl}=a(1+\delta)^2+\frac{h}{4}, \quad (7)$$

$$Q=a(1+\delta)\delta-\frac{h}{4}. \quad (8)$$

A mesoscopic state of the sample is given by the series $\{\hat{s}(\mathbf{x})\}$, where $\hat{s}(\mathbf{x})$ assumes a particular value (1, −1, or 0) in each cell. The probability of a particular mesoscopic state is given by

$$p[\{\hat{s}(\mathbf{x})\}]=\Xi^{-1}e^{-\beta\mathcal{H}}, \quad (9)$$

with

$$\Xi=\sum_{\{\hat{s}(\mathbf{x})\}}e^{-\beta\mathcal{H}}, \quad (10)$$

where the sum runs over all mesoscopic states $\{\hat{s}(\mathbf{x})\}$.

The grand-thermodynamic potential is given by the standard statistical-mechanics formula

$$\Omega = -pv_0V = -kT \ln \Xi, \tag{11}$$

where p is pressure, V is the number of lattice cells, and v_0V is volume. In the case of waterlike substance there is no direct way of measuring $\langle \hat{s} \rangle$ and $\langle \hat{s}^2 \rangle$ separately; the only measurable quantity is density. The density of water in this model is given by $\langle \rho \rangle = \bar{\rho} \rho_{LDW}$, with

$$\bar{\rho} = \langle \rho \rangle / \rho_{LDW} = [(1+\delta)\langle \hat{s}^2 \rangle + \delta \langle \hat{s} \rangle] = -\left. \frac{\partial \beta \Omega}{\partial \beta \mu(\mathbf{x})} \right|_{\mu(\mathbf{x})=\mu}, \tag{12}$$

where $\langle \cdots \rangle$ denotes the average with the probability (9); we replaced μ by the cell-dependent chemical potential $\mu(\mathbf{x})$ in (5) and used (11). The (rescaled) density-density correlation function $G_{\rho\rho}$ is defined by

$$G_{\rho\rho}(\mathbf{x}_1 - \mathbf{x}_2) = \langle [(1+\delta)\hat{s}^2(\mathbf{x}_1) + \delta \hat{s}(\mathbf{x}_1)][(1+\delta)\hat{s}^2(\mathbf{x}_2) + \delta \hat{s}(\mathbf{x}_2)] \rangle - \bar{\rho}^2 = -\left. \frac{\partial^2 \beta \Omega}{\partial \beta \mu(\mathbf{x}_1) \partial \beta \mu(\mathbf{x}_2)} \right|_{\mu(\mathbf{x}_i)=\mu}. \tag{13}$$

In the following sections we analyze three limiting cases: $T \to 0$; next, the case of high density and finally the case of low density. In these limiting cases the model can be simplified. The simplified versions of the model can be solved or compared to previously found solutions. By analyzing the results of the simplified versions of the model, we can find for what ranges of the model parameters the waterlike behavior can be found. By requiring the consistency of the calculated quantities with the known results for water, we can find the best choice of parameters.

III. PROPERTIES OF THE MODEL

A. Ground state

Let us first focus on the low-temperature properties of the model and find the conditions corresponding to the stability of different states and to the phase equilibria. For $T \to 0$ the probability (9) becomes very narrow, and at $T=0$ the probability that any state different from the ground state appears vanishes. When only the ground-state contributes to Ξ in (10) and μ is fixed, then $\Omega = \min(\mathcal{H})$. Whether the $\mathcal{H}$ assumes a minimum for the state 1, 2, or 3 depends on the parameters. We shall calculate $\mathcal{H}$ for three uniform states: $\hat{s}=1$, $\hat{s}=-1$, or $\hat{s}=0$ in each cell. The first two states represent the close-packed and tetrahedral condensed phases, respectively, and $\hat{s}=0$ represents the vapor. Note that at $T=0$ the density of vapor tends to zero. Note also that in the lattice-gas models there is no transition between liquid and crystalline phases, because it is not possible to distinguish between long- and short-range order in the condensed state. We are not interested in the stable crystalline, but in the metastable liquid phases; therefore, for our purposes this deficiency of lattice models is in fact an advantage. By comparing the value of $\mathcal{H}$ for $\hat{s}=1$, $\hat{s}=-1$, and $\hat{s}=0$, we can find the regions in the parameter space (a,h,δ,μ) corresponding to the stability of the three phases. From Eq. (2) we obtain

$$\mathcal{H} = \begin{cases} -(1+2\delta)[3(1+2\delta)a + \mu]V & \text{if } \hat{s}=1, \\ -[3(a+h)+\mu]V & \text{if } \hat{s}=-1, \\ 0 & \text{if } \hat{s}=0. \end{cases} \tag{14}$$

The coexistence between two phases is obtained by equating the values of $\mathcal{H}$ in these phases. In this way we find that the coexistence between the $s=0$ and $s=-1$ phases occurs for

$$\frac{\mu}{a} = -3\left(1 + \frac{h}{a}\right). \tag{15}$$

At the coexistence between the $s=1$ and $s=-1$ phases we have

$$\frac{\mu}{a} = -6(1+\delta) + \frac{3h}{2a\delta}. \tag{16}$$

Finally, the coexistence between the $s=0$ and $s=1$ is given by

$$\frac{\mu}{a} = -3(1+2\delta). \tag{17}$$

All three phases can coexist at a triple point if the hydrogen-bond and vdW energies are such that $h=2\delta a$. The dependence of the $T=0$ phase diagram on the parameter ratio h/a is shown in Fig. 2.

For $h<2\delta a$ a transition between vapor (vacuum) and high-density ($s=1$) phases occurs at $\mu/a=-3(1+2\delta)$. For $h<2\delta a$ the system does not exhibit the transition between the two (metastable) liquid phases. For $h>2\delta a$ there is the transition between vacuum and the low-density phase for $\mu/a=-3(1+h/a)$ and, next, the transition between the low- and high-density phases for $\mu/a=-6(1+\delta)+3h/(2\delta a)$. Such a coexistence between two metastable liquid phases is hypothesized for water. Thus, for parameters that satisfy the condition

$$\frac{h}{a} > 2\delta, \tag{18}$$

the waterlike behavior can be expected in this model.

The value of $\mathcal{H}$ at the coexistence between the two dense phases, $\hat{s}=1$ and $\hat{s}=-1$, can be obtained by inserting (16) into (14). Because for $T \to 0$ we have $\Omega \to \mathcal{H}$, we obtain from (11) the pressure at the coexistence between the two liquid phases for $T \to 0$:

$$p_{coex}v_0 = 3(1+2\delta)\left(\frac{h}{2\delta} - a\right), \quad T \to 0. \tag{19}$$

By equating the left-hand side (LHS) of the above equation to the value expected for real water, we obtain the first relation between the model parameters. The anomalous and normal properties of water are observed for $p<p_0$ and for $p>p_0$, respectively, where $p_0 \approx 2000$ bars. We assume that $p_{coex} \approx p_0$ at the coexistence between the two metastable liquid phases for $T \to 0$.

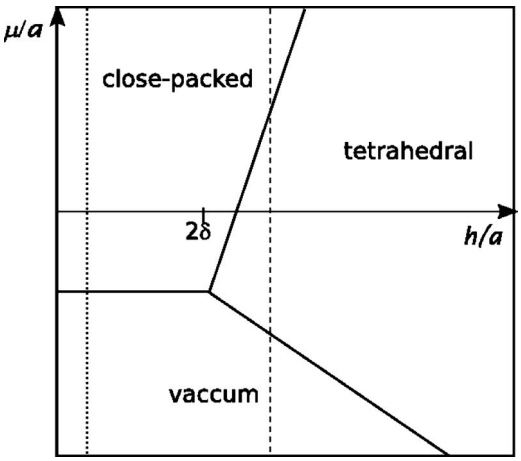

FIG. 2. The ground-state dependence on the model parameters a, h, and δ and on the chemical potential μ. Regions corresponding to stability of different phases (close-packed, tetrahedral, and vacuum) at $T=0$ are indicated, and the solid lines between stability regions of two phases represent the corresponding phase coexistence. Different values of the ratio between the H-bond and vdW energies, h/a, correspond to different substances. The dotted and dashed lines represent examples of the ground-state dependence on μ for two substances showing qualitatively different behavior. Along the dotted line the vapor and close-packed phases are stable for $\mu/a \leqslant -3(1+2\delta)$ and $\mu/a \geqslant -3(1+2\delta)$, respectively. Such "normal" behavior is found for $h/a < 2\delta$. Along the dashed line the vapor and close-packed phases are stable for low $[\mu/a \leqslant -3(1+h/a)]$ and high $[\mu/a \geqslant -6(1+\delta)+3h/(2\delta a)]$ values of μ/a, respectively, while for $-3(1+h/a) \leqslant \mu/a \leqslant -6(1+\delta)+3h/(2\delta a)$ the tetrahedral condensed phase is found. The stability of the tetrahedral condensed phase that characterizes waterlike systems is found for parameters that satisfy the inequality $h/a > 2\delta$.

B. Model in the case of high ρ

In the limiting case of high densities we can reduce the model to a simplified version by eliminating the states $\{\hat{s}(\mathbf{x})\}$ that occur with very low probability. In the high-density case the empty cells are very rare, and the mesoscopic states with $\hat{s}=0$ can be neglected in calculating the average quantities. In that case $\hat{s}=1,-1$, and by inserting $\hat{s}^2=1$ into Eq. (5) we end up with the Ising model

$$\mathcal{H}^{ll} = -\sum_{\mathbf{x}}\sum_{i} J^{ll}\hat{s}(\mathbf{x})\hat{s}(\mathbf{x}+\mathbf{e}_i) - H_1^{ll}\sum_{\mathbf{x}}\hat{s}(\mathbf{x}) - H_0^{ll}\sum_{\mathbf{x}} 1, \tag{20}$$

where

$$H_1^{ll} = 6Q + \delta\mu \tag{21}$$

and

$$H_0^{ll} = 12J^{gl} + (1+\delta)\mu. \tag{22}$$

The critical temperature in the Ising model is known from simulations, and its value is $kT_c \approx 4.5J^{ll}$. From this result and from (6) we have

$$T_c^{ll} \approx \frac{4.5J^{ll}}{k} = \frac{4.5}{k}\left(a\delta^2 + \frac{h}{4}\right). \tag{23}$$

By assuming that the LHS of (23) is equal to the temperature at the critical point of the metastable liquid-liquid separation in water, we obtain the second relation between the model parameters. The phase coexistence in the Ising model occurs for $H_1^{ll}=0$, and from (21) we obtain the chemical potential at the liquid-liquid coexistence (including the critical point), $\mu_c = -6Q/\delta$.

C. Model in the case of low ρ

Let us focus on the case of low densities. There is no distinction between structured and unstructured water, when the NNs of an occupied cell are typically empty, as in the gas or supercritical phase. We assume that we can average over $\hat{s}$ in the Hamiltonian (5). The average value of $\hat{s}$ is zero. For $\hat{s}=0$ and $\hat{s}^2=0,1$ we have

$$\mathcal{H}_{gl} = -\sum_{\mathbf{x}}\sum_{i} 4J^{gl}\hat{s}^2(\mathbf{x})\hat{s}^2(\mathbf{x}+\mathbf{e}_i) + -\mu\sum_{\mathbf{x}}(1+\delta)\hat{s}^2(\mathbf{x}). \tag{24}$$

By changing the variables,

$$\hat{s}^2 = \frac{\hat{\sigma}+1}{2}, \tag{25}$$

we again obtain the Ising model

$$\mathcal{H}^{gl} = -\sum_{\mathbf{x}}\sum_{i} J^{gl}\hat{\sigma}(\mathbf{x})\hat{\sigma}(\mathbf{x}+\mathbf{e}_i) - H_1^{gl}\sum_{\mathbf{x}}\hat{\sigma}(\mathbf{x}) - H_0^{gl}\sum_{\mathbf{x}} 1, \tag{26}$$

with

$$H_1^{gl} = 6J^{gl} + \frac{1+\delta}{2}\mu, \tag{27}$$

$$H_0^{gl} = 3J^{gl} + \frac{1+\delta}{2}\mu. \tag{28}$$

The chemical potential at the critical point and along the phase coexistence is given by $H_1^{gl}=0$ and $\mu_c = -12J^{gl}/(1+\delta)$. We again use the simulation result for the temperature at the critical point in the Ising model, and from (7) we obtain

$$T_c^{gl} \approx \frac{4.5J^{gl}}{k} = \frac{4.5}{4k}\left[a(1+\delta)^2 + \frac{h}{4}\right]. \tag{29}$$

By equating the LHS of the above to the temperature at the gas-liquid critical point in water, we obtain the third relation between the model parameters.

D. Model parameters for water

Note that in water the temperature of the gas-liquid critical point is much higher than the temperature of the metastable liquid-liquid critical point. We should thus require that in waterlike substance $T_c^{gl} \gg T_c^{ll}$. The above condition and (18)

give together the range of h/a for which the model can exhibit similar properties as real water

$$2\delta < \frac{h}{a} \ll \frac{4(1+3\delta)(1-\delta)}{3}. \tag{30}$$

From (23) and (29) we obtain

$$a = a_0 k, \quad a_0 = \frac{4T_c^{gl} - T_c^{ll}}{4.5(1+2\delta)}, \tag{31}$$

$$h = h_0 k, \quad h_0 = 4\frac{(1+\delta)^2 T_c^{ll} - 4\delta^2 T_c^{gl}}{4.5(1+2\delta)}. \tag{32}$$

We assume

$$T_c^{gl} = 650 \text{ K}, \quad T_c^{ll} = 180 \text{ K}, \quad p_{coex} = 1900 \text{ bars}. \tag{33}$$

From the above and Eqs. (31), (32), and (19) we obtain a relation between v_0 and δ. Choosing $v_0 = 35$ Å^3, we obtain $\delta = 0.12$, $a_0 = 433.7$ K ($a = 598.5 \times 10^{-23}$ J $= 3.6$ kJ/mol), $h_0 = 135.02$ K ($h = 186 \times 10^{-23}$ J $= 1.2$ kJ/mol). These values are in semiquantitative agreement with the water parameters. The H-bond energy is small compared to the value 23 kJ/mol, but in the mesoscopic model we do not consider the individual bond, but rather the interaction energy averaged over different orientations and distances between the molecules. Note that there are four NNs in the tetrahedral structure and six NNs on the simple cubic lattice. The H bond is strongly directional, and by averaging over all orientations we obtain

$$\frac{4 \times 23 \text{ kJ/mol}}{6 \times 4\pi} \approx 1.83 \text{ kJ/mol}. \tag{34}$$

Note that we could fix the model parameters based on experimental values. However, the presence of the lattice structure changes the value of the critical temperature for given energy parameters; therefore, we proceeded in the way described above.

IV. RESULTS IN THE MEAN-FIELD APPROXIMATION

The BEG model was first solved in Ref. [36] in the MF approximation. Details of our version of the MF approximation can be found for example in Refs. [33,36]. In the MF approximation the equation of state, the spinodal line, and the transitions between uniform phases are correctly described on a qualitative level. However, when fluctuations are included beyond the MF approximation, the stability region of the disordered phase enlarges. Thus, the critical-point temperature obtained in the MF approximation, T_c^{MF}, is overestimated. In the case of the Ising model, $T_c/T_c^{MF} \approx 3/4$. Also, fluctuations yield a positive contribution to the grand potential $\Omega = -pv_0$; therefore, the MF result for pressure, p^{MF}, is overestimated as well. Another important source of inaccuracy of the quantitative results of the model is the underlying lattice. In particular, the symmetrical shape of the gas-liquid coexistence line, resulting from the underlying lattice, differs significantly from the shape of the corresponding line in real systems. The above features should be taken into account when comparing the MF results with experiments. Since the MF approximation for the BEG model is well known, we describe only the main steps of derivation of the equation of state, the spinodal line, and the phase diagram. The density-density correlation function is calculated in the Gaussian approximation.

In the MF approximation the grand potential (11) is approximated by the minimum with respect to η and s of the functional

$$\Omega^{MF}[s(\mathbf{x}), \eta(\mathbf{x})] = \mathcal{H}[s(\mathbf{x}), \eta(\mathbf{x})] - TS[s(\mathbf{x}), \eta(\mathbf{x})], \tag{35}$$

where the entropy on the lattice has the form

$$S[s(\mathbf{x}), \eta(\mathbf{x})] = -k\sum_{\mathbf{x}} \left[\frac{\eta(\mathbf{x}) + s(\mathbf{x})}{2} \ln\left(\frac{\eta(\mathbf{x}) + s(\mathbf{x})}{2} \right) + \frac{\eta(\mathbf{x}) - s(\mathbf{x})}{2} \ln\left(\frac{\eta(\mathbf{x}) - s(\mathbf{x})}{2} \right) + [1 - \eta(\mathbf{x})] \ln[1 - \eta(\mathbf{x})] \right], \tag{36}$$

and $\mathcal{H}[s(\mathbf{x}), \eta(\mathbf{x})]$ is given in Eq. (5) with $\hat{s}$ and $\hat{s}^2$ replaced by s and η, respectively. $0 \leqslant \eta \leqslant 1$ is the fraction of occupied cells and is analogous to the number density in a mixture isomorphic to our model. Here $-1 \leqslant s = 2x - 1 \leqslant 1$, and x is analogous to the concentration of one species (locally disordered water) in the corresponding mixture. In order to simplify the notation we rewrite Eq. (12) in the form

$$\bar{\rho} = \frac{\langle \rho \rangle}{\rho_{LDW}} = (1+\delta)\eta + \delta s. \tag{37}$$

For uniform phases Eq. (35) assumes the explicit form

$$\Omega^{MF}(s, \eta)/V = -pv_0 = -\{3J^{ll}s^2 + 12J^{gl}\eta^2 + 6Qs\eta + \mu[\delta s + (1+\delta)\eta]\} - Ts_V, \tag{38}$$

where we used Eq. (5) and where

$$s_V = -k\left[\frac{\eta + s}{2} \ln\left(\frac{\eta + s}{2} \right) + \frac{\eta - s}{2} \ln\left(\frac{\eta - s}{2} \right) + (1 - \eta)\ln(1 - \eta) \right] \tag{39}$$

is the entropy per lattice cell. The explicit forms of the minimum conditions,

$$\frac{\partial \Omega^{MF}}{\partial s} = 0, \tag{40}$$

$$\frac{\partial \Omega^{MF}}{\partial \eta} = 0, \tag{41}$$

are given in Appendix A.

A. Spinodal line and phase diagram

The function $\Omega^{MF}(s, \eta)$ assumes a minimum for s and η satisfying Eqs. (40) and (41) when its second derivative is positive definite. The boundary of stability is given by

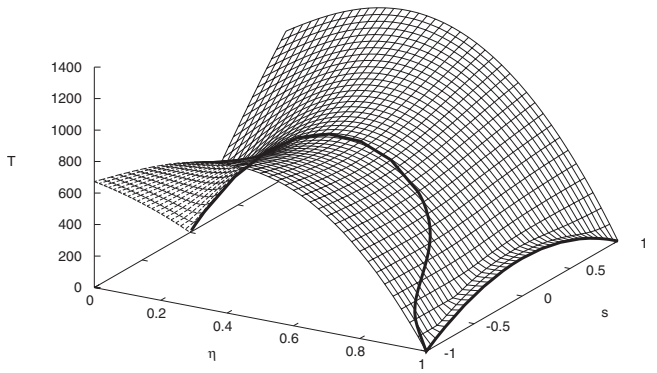

FIG. 3. The spinodal surface $T=T_s(\eta,s)$ as a function of s and η. The s and η are not independent in equilibrium states, and in the MF approximation the relation between them is given in Eq. (43). The cross section of the surface $T=T_s(\eta,s)$ with the surface (43) is shown as the thick line. This line together with Eq. (37) gives the spinodal line that represents the loci of the actual instability of the model system in the (ρ, T) diagram. T is in kelvins; s and η are dimensionless.

$$\det[\partial^2 \beta\Omega^{MF}] = 0, \tag{42}$$

where $\partial^2 \beta\Omega^{MF}$ is the matrix of the second derivative of $\beta\Omega^{MF}$ with respect to η and s. The rather lengthy explicit expression for $T=T_s(\eta,s)$, following from Eq. (42), is given in Appendix A [Eq. (A3)], and the surface $T=T_s(\eta,s)$ is shown in Fig. 3.

In equilibrium η and s are not independent, and the relation between them [Eqs. (40) and (41) and Eqs. (A1) and (A2) in Appendix A] is given by

$$\left[\frac{kT}{2}\ln\left(\frac{\eta+s}{\eta-s}\right) - 6J^{ll}s - 6Q\eta\right](1+\delta) = \left[\frac{kT}{2}\ln\left(\frac{\eta^2-s^2}{4(1-\eta)^2}\right) - 24J^{gl}\eta - 6Qs\right]\delta. \tag{43}$$

The spinodal line in the (ρ, T) phase diagram is given as a parametric equation in Eqs. (A3), (A6), and (37) and is shown in Fig. 4. More calculation details are given in Appendix A.

From the simplified versions of the model (Secs. III B and III C) we can obtain the approximate forms of the spinodal line. For low density we assume $s=0$—i.e., the density is $\bar{\rho}=(1+\delta)\eta$—and we obtain the approximate form of the spinodal (see Sec. III C):

$$kT = 24J^{gl}\eta(1-\eta) = 24J^{gl}\frac{\bar{\rho}(1+\delta-\bar{\rho})}{(1+\delta)^2}. \tag{44}$$

The above form is valid only for $\eta \ll 1$. For high density we assume $\eta=1$—hence $\bar{\rho}=(1+\delta)+\delta s$—and consider the simplified model described in Sec. III B. The spinodal for the model (20) assumes the form

$$kT = 6J^{ll}(1-s^2) = \frac{6J^{ll}}{\delta^2}\{\bar{\rho}[2(1+\delta)-\bar{\rho}]-1-2\delta\}. \tag{45}$$

Equations (44) and (45) represent the intersection of the surface $T=T_s(\eta,s)$ with the planes $s=0$ and $\eta=1$, respectively.

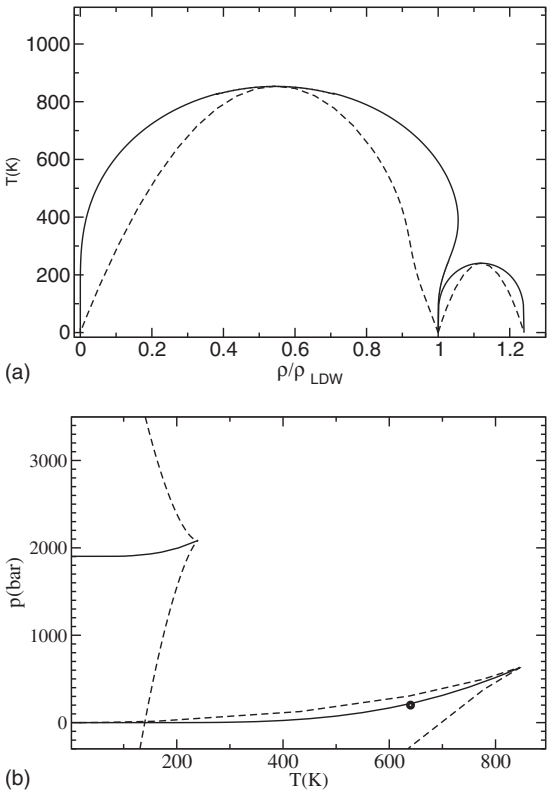

FIG. 4. Spinodal (dashed) and binodal (solid) lines in the MF approximation. The symbol shows the experimental critical point of water. Note that exact values of the critical temperatures in this model are expected to be $T_c \approx 0.75 T_c^{MF}$. ρ/ρ_{LDW} is dimensionless; ρ_{LDW} is the model parameter, and its order of magnitude is $\rho_{LDW} \sim \rho_{ice} \approx 0.9$ g/cm^3.

For $\eta \to 1$ the approximation (44) fails, because from (43) it follows that when $\eta \to 1$, then $s \to -1$ at the gas-liquid branch of the spinodal (see Fig. 3). Water anomalies result from this failure of the simple lattice-gas model. On the other hand, Eq. (45) is a good approximation; it almost coincides with the results of the full model.

The phase equilibria shown in Fig. 4 are obtained by equating the values of p [Eq. (38)] and μ [Eqs. (40) and (41)] for two phases α and β characterized by the pair of variables (η_α, s_α) and (η_β, s_β). For more details, see Appendix B.

In the simplified versions of the model (Secs. III B and III C) we obtain the simple expressions

$$kT = \frac{12J^{gl}[2\bar{\rho}-(1+\delta)]}{(1+\delta)[\ln(\bar{\rho})-\ln(1+\delta-\bar{\rho})]} \tag{46}$$

and

$$kT = \frac{12J^{ll}[\bar{\rho}-(1+\delta)]}{\delta[\ln(\bar{\rho}-1)-\ln(1+2\delta-\bar{\rho})]} \tag{47}$$

for the gas-liquid and the liquid-liquid transition, respectively. As in the case of the spinodal, Eq. (46) is reasonably good at the gas branch and fails at the liquid branch of the gas-liquid coexistence. The approximation (47) for the

liquid-liquid branch cannot be distinguished from the exact MF result in Fig. 4.

Note that the slope of the liquid-liquid coexistence line $p(T)$ is very small, but positive, contrary to the common expectation that the entropy per mole in the LDW is lower than the entropy in the HDW. We verified that in the MF approximation $p_{coex}<p_c^{ll}$ for $0.05<\delta<0.2$, where p_{coex} is pressure at the coexistence at very low T [see (19)] and p_c^{ll} is pressure at the critical point of the liquid-liquid coexistence. Thus, $dp(T)/dT>0$ is the property of the MF solution of the model for the relevant range of parameters. At the present stage we are not able to verify if beyond the MF approximation the slope of the coexistence line remains positive. As already mentioned, fluctuations usually lead to lower values of pressure and the fluctuation contribution increases with increasing temperature. We can expect that exact solution for the coexistence line in this model should correspond to a smaller slope of the line $p(T)$, and since this slope is very small in the MF approximation, no definite conclusions concerning the sign of $dp(T)/dT$ can be drawn before reliable simulations are performed. In any case, even if it turns out that beyond the MF approximation $dp(T)/dT<0$ in this model, its magnitude is expected to be much smaller than in other models where orientational degrees of freedom are explicitly included [13,16,18,29]. We stress that our model shows that the difference in the entropy associated with the local ordering in the LDW and HDW is not necessary for obtaining the density anomaly. This is reminiscent to the presence of the density anomaly in the ramp model, where interactions are independent of orientations [22,24].

B. Equation of state, thermal expansion, and heat capacity

The equation of state (EOS) in (μ, p, T) variables is given in Eq. (38), with η and s eliminated with the help of Eqs. (40) and (41). In order to obtain the EOS in the ρ, p, and T variables, we eliminate μ from (38) by using (40), and by subsequent use of Eqs. (40) and (41) we obtain the simple form, valid for $\eta<1$,

$$pv_0 = -3J^{ll}s^2 - 12J^{gl}\eta^2 - 6Q\eta s - kT\ln(1-\eta). \quad (48)$$

The EOS in the (ρ, p, T) variables is given in Eq. (48), with s and η expressed in terms of $\bar{\rho}$ and T by solving Eqs. (43) and (37). Some calculation details are given in Appendix C. The plots of the isobars $T(\rho)$ for $p=10$, 100, 653, 1000, 1950, 2085, and 2500 bars are shown in Fig. 5. Note that the shape of the isobars for $p_{coex}<p<p_c^{ll}$ results from the positive slope of the liquid-liquid coexistence line $p(T)$ in our simple MF approximation.

In the asymptotic cases of very low and very high density, the EOS assumes simpler forms that can be obtained from the simplified versions of the model described in Secs. III B and III C. Let us first describe the case of low density. By assuming $s=0$, we obtain $\bar{\rho}=(1+\delta)\eta$ and

$$pv_0 + \frac{12J^{gl}}{(1+\delta)^2}\bar{\rho}^2 = -kT\ln\left(1-\frac{\bar{\rho}}{1+\delta}\right), \quad (49)$$

which is the lattice-gas version of the vdW EOS. Note that the RHS of Eq. (49) diverges for $\bar{\rho}\to 1+\delta$; therefore, for large densities pressure is significantly overestimated. This well-known deficiency of the lattice-gas models results from the hole-particle symmetry on the lattice, which in real systems is absent.

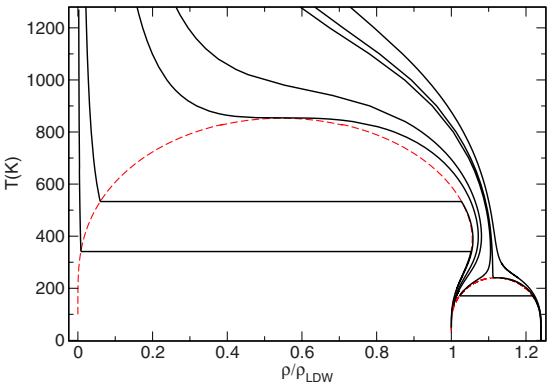

FIG. 5. (Color online) $T(\rho)$ isobars (solid lines). From the left to the right lines $p=10$, 100, 653, 1000, 1950, 2085, and 2500 bar. The dashed lines are the phase transitions. The critical pressures for the gas-liquid and liquid-liquid transitions are $p_c^{gl}\approx 653$ bars and $p_c^{ll}\approx 2085$ bars, respectively. In the MF approximation the extent of the two-phase regions and pressure are both overestimated compared to exact results. In addition, the pressure is overestimated due to the lattice structure. The exact values of the critical temperatures are expected to be $T_c\approx 0.75T_c^{MF}$. T is in kelvins, and ρ/ρ_{LDW} is dimensionless; ρ_{LDW} is the model parameter, and its order of magnitude is $\rho_{LDW}\sim\rho_{ice}\approx 0.9$ g/cm^3.

For high density we assume $\eta=1$ and consequently $\bar{\rho}=(1+\delta)+\delta s$ (see Sec. III B). The EOS for high densities takes the form [see (38) and (40)]

$$kT\mathcal{L}(\bar{\rho}) = pv_0 + \mathcal{R}(\bar{\rho}), \quad (50)$$

where

$$\mathcal{L}(\bar{\rho}) = \left(\frac{1}{2\delta}\ln(\bar{\rho}-1) - \frac{1+2\delta}{2\delta}\ln(1+2\delta-\bar{\rho}) + \ln(2\delta)\right) \quad (51)$$

and

$$\mathcal{R}(\bar{\rho}) = \frac{3J^{ll}}{\delta^2}\bar{\rho}^2 + 6Q\frac{1+\delta}{\delta} - 12J^{gl} - 3J^{ll}\left(\frac{1+\delta}{\delta}\right)^2. \quad (52)$$

The critical pressure is given by $p_cv_0=kT_c\mathcal{L}(\bar{\rho}_c)-\mathcal{R}(\bar{\rho}_c)\approx 2085$ bars, where $T_c\approx 240$ K and $\bar{\rho}_c=1+\delta$ are obtained from Eq. (45). Note that $\mathcal{L}(\bar{\rho}_0)=0$ for $\bar{\rho}_0\approx 1.111$ and the pressure $p_0=-\mathcal{R}(\bar{\rho}_0)/v_0\approx 2084$ bars is independent of T. For $p>p_0$, $T(\bar{\rho})$ given in Eq. (50) decreases from $T(\bar{\rho}_0)=\infty$ for $\bar{\rho}$ *increasing* from $\bar{\rho}_0$, whereas for $p<p_0$, $T(\bar{\rho})$ decreases from $T(\bar{\rho}_0)=\infty$ for $\bar{\rho}$ *decreasing* from $\bar{\rho}_0$. Hence, p_0 is the borderline value separating the normal [negative slope of $T(\rho)$] from the anomalous [positive slope of $T(\rho)$] density behavior for $p>p_0$ and $p<p_0$, respectively. The density $\bar{\rho}_0\approx 1.111$ is the maximum density for $p<p_0$. Note that in the simplified model (Sec. III B) no holes are present, so its validity is limited to relatively low T. At higher T the negative slope of $T(\rho)$ is found in the full model, as seen in Fig. 5.

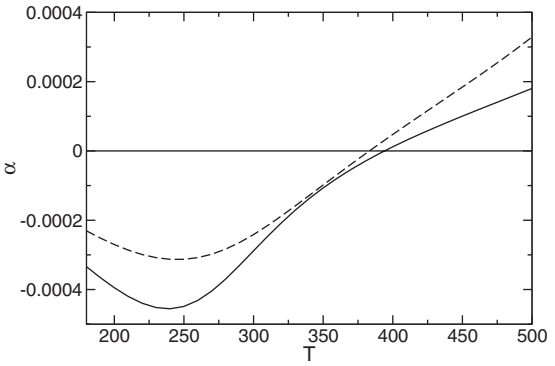

FIG. 6. Thermal expansivity (53) for $p=100$ bars (dashed line) and $p=1000$ bars (solid line); T is in kelvins. α is in inverse kelvins. Beyond the MF approximation we expect a shift of the plot towards lower T values.

Since for $\eta=1$ there are no empty cells, the EOS (50) shows no singularity for $\bar{\rho}=1+\delta$. On the other hand, $|\mathcal{L}(\bar{\rho})| \to \infty$ for $\bar{\rho}\to 1$ and $\bar{\rho}\to 1+2\delta$. Therefore we expect significantly overestimated pressures for $\bar{\rho}\to 1$ and $\bar{\rho}\to 1+2\delta$.

The thermal expansivity

$$\alpha = -\frac{1}{\bar{\rho}}\frac{\partial\bar{\rho}}{\partial T}\bigg|_p \tag{53}$$

can be obtained by direct differentiation of the isobars shown in Fig. 5 and is shown in Fig. 6 for $p=100$ and 1000 bars. As expected from the shape of the isobars, we obtain the characteristic anomalous negative expansivity for the relevant range of temperature.

The isobaric heat capacity is given by

$$c_P = T\frac{\partial(s_V N_A/\bar{\rho})}{\partial T}\bigg|_p, \tag{54}$$

where $s_V N_A/\bar{\rho}$ is the molar entropy, with the entropy per cell s_V given in Eq. (39) (ideal entropy of mixing), and N_A is the Avogadro number. The isobaric heat capacity is shown in Fig. 7 for $p=100$ and 1000 bars. Note the increase of the heat capacity upon cooling at constant pressure for the relevant range of temperatures, in agreement with the anomalous behavior of water. Recall that in calculating the entropy we disregarded the difference in the entropy of *local* ordering in the locally ordered and locally disordered water (cells with $\hat{s}=-1$ and $\hat{s}=1$, respectively). Evidently, the anomalous heat capacity results from the entropy associated with different spatial distributions of the locally ordered and locally disordered regions, rather than from the entropy associated with local ordering in regions on the molecular length scale.

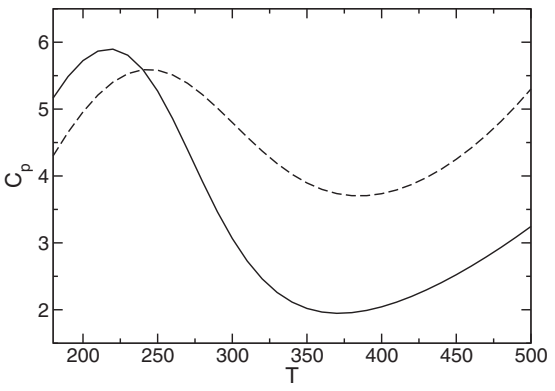

FIG. 7. Isobaric heat capacity (54) for $p=100$ bars (dashed line) and $p=1000$ bars (solid line). T is in kelvins (K); c_p is in J/K/mol. Beyond the MF approximation we expect a shift of the plot towards lower T values.

C. Density-density correlation function and the compressibility

The density-density correlation function (13) can be written in the form

$$G_{\rho\rho} = (1+\delta)^2 G_{\eta\eta} + \delta^2 G_{ss} + 2\delta(1+\delta)G_{\eta s}, \tag{55}$$

where according to standard rules $G_{\alpha\beta}=[\mathbf{C}]^{-1}_{\alpha\beta}$, with $[\mathbf{C}]$ denoting the matrix of the second derivative of the function $\beta\Omega^{MF}(s,\eta)$. The explicit form of $[\mathbf{C}]$ in Fourier representation is

$$\tilde{C}_{\eta\eta}(\mathbf{k}) = \frac{\eta}{\eta^2 - s^2} + \frac{1}{1-\eta} - 4J^{gl}Z, \tag{56}$$

$$\tilde{C}_{\eta s}(\mathbf{k}) = -\frac{s}{\eta^2 - s^2} - QZ, \tag{57}$$

$$\tilde{C}_{ss}(\mathbf{k}) = \frac{\eta}{\eta^2 - s^2} - J^{ll}Z, \tag{58}$$

where we introduced $Z=2\beta\Sigma_{i=1}^{3}\cos(k_i)$ and $\mathbf{k}=(k_1,k_2,k_3)$. Standard algebra yields the expressions

$$\tilde{G}_{ss}(\mathbf{k}) = \frac{\eta - s^2 - 4J^{gl}(\eta^2 - s^2)(1-\eta)Z}{1 + A_{D1}Z + A_{D2}Z^2}, \tag{59}$$

$$\tilde{G}_{\rho\rho}(\mathbf{k}) = \frac{A_{N0} + A_{N1}Z}{1 + A_{D1}Z + A_{D2}Z^2}, \tag{60}$$

where the coefficients A_{Ni} and A_{Di} are given in Appendix C. Their values should be calculated for s and η, which satisfy the equilibrium condition (43).

The results of the lattice models for fluids are meaningful for distances much larger than the lattice constant, where the lattice structure is irrelevant. For $k\to 0$ we have $Z=\beta[6-k^2+O(k_i^2k_j^2)]$, where $k^2=\Sigma_{i=1}^{3}k_i^2$, and up to $O(k^2)$ Eqs. (59) and (60) show no anisotropy resulting from the lattice structure:

$$\tilde{G}_{ff}(\mathbf{k}) \simeq \frac{A_{ff}}{(\xi_{ff}^{-2} + k^2)}, \quad k\to 0, \tag{61}$$

where f denotes s or ρ. The correlation function $G_{ss}(\mathbf{k})$ is analogous to the correlation function for concentration fluctuations in binary mixtures. The region of excess concentration of one component in this model is analogous to the cluster of H-bonded molecules. The average spatial extent of the "cluster" is of the order of the correlation length for the concentration of the locally ordered (or disordered) component.

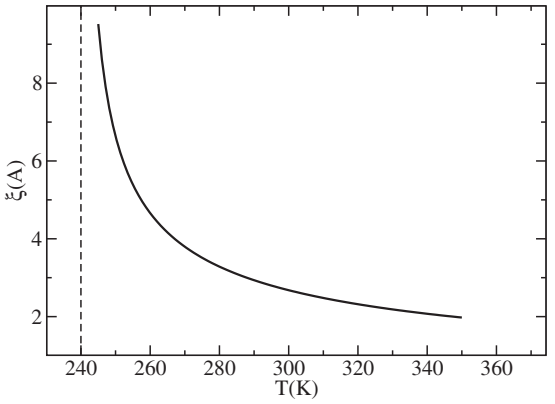

FIG. 8. The correlation length for $\eta=1$ and $s=0$. ξ is in angstroms; T is in kelvins. In our MF approximation, $T_c^{MF}\approx 240$ K (dashed line).

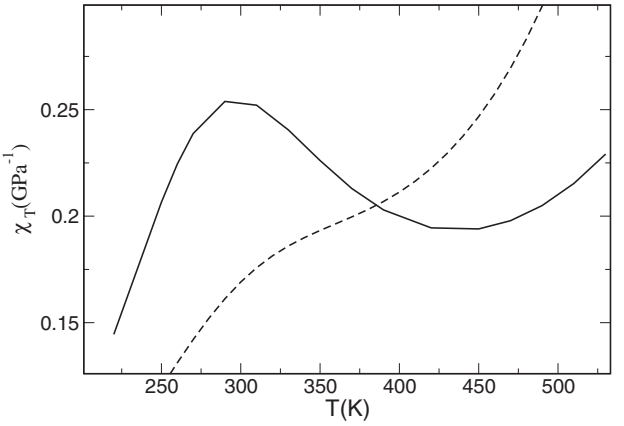

FIG. 9. Compressibility as a function of temperature for $p=1000$ bars (solid line) and $p=100$ bars (dashed line). T is in kelvins; χ_T is in GPa^{-1}.

For $\eta=1$ and $s=0$ the correlation functions assume the simple form

$$\tilde{G}_{\rho\rho}(\mathbf{k}) = \delta^2 \tilde{G}_{ss}(\mathbf{k}) \simeq \delta^2 \frac{kT/J^{ll}}{(\xi^{-2}+k^2)}, \quad k \to 0, \tag{62}$$

and in real space

$$rG_{ss}(r) \simeq \frac{kT}{4\pi J^{ll}} e^{-r/\xi}. \tag{63}$$

The correlation length

$$\xi = \xi_{ss} = \xi_{\rho\rho} = \sqrt{kT/J^{ll} - 6} \tag{64}$$

is shown in Fig. 8 as a function of T. The above approximate forms are valid for the parameter range where the empty cells are very rare—i.e., for high densities and low temperatures.

The isothermal compressibility in ρ and T variables is given by

$$\chi_T = \frac{1}{\rho}\frac{\partial \rho}{\partial p} = \frac{\tilde{G}_{\rho\rho}(0)v_0}{kT\bar{\rho}^2} = \frac{A_{N0}kT + 6A_{N1}}{(kT)^2 + 6A_{D1}kT + 36A_{D2}} \frac{v_0}{\bar{\rho}^2}, \tag{65}$$

where χ_T as a function of T and p can be obtained by eliminating η and s from (65) with the help of (43) and (48). The result is shown in Fig. 9 for $p=100$ and 1000 bars. The anomalous behavior of the isothermal compressibility is found in this model only for high pressures (but lower than $p_0\approx 2000$ bars). As discussed in the context of the EOS, pressure is significantly overestimated in the lattice models.

V. SUMMARY

We have introduced a very simple, three-state lattice model for waterlike fluid. The model is a special version of the BEG model [36]. Water is treated as a mixture of two components, whose chemical potentials are *not* independent. One component represents locally ordered and the other one locally disordered water. It is assumed that the density of the disordered component is larger, and the ratio between the chemical potentials is given by the density ratio $1+2\delta$. Interaction potentials of the van der Waals type are proportional to the common parameter a and to the product of densities of the interacting species. In addition, the H-bond interaction h is assumed for the component representing the locally ordered water. The liquid-liquid critical point in this model is identified with the critical point of the demixing transition in the corresponding mixture. We fix the model parameters by requiring that the critical points for the gas-liquid and demixing transition coincide with the experimental values and the demixed components coexist at very low temperature for $p=1900$ bars. There are thus three relations between four model parameters δ, a, h, and the volume per particle in the ice structure, v_0. We arbitrarily choose the volume per particle in the ice structure, $v_0=35$ Å^3. The chosen parameters are in semiquantitative agreement with experimental values.

We solve the model in mean-field approximation. The shape of the gas-liquid coexistence line (Fig. 4) is in qualitative agreement with earlier theoretical and experimental results [16,18]. The maximum-density temperature, however, is too high compared to real water. The shape of the phase-coexistence lines depends on the model parameters, especially on δ, but we did not attempt to find the best choice of parameters. Improvement of the quantitative results is expected beyond the simple MF approximation. Note that in Ref. [16] water anomalies *are not found* on the same MF level as in our case. The anomalous density increase with temperature for $p<p_0\approx 2084$ bars in this model is explained as follows. For low T and $p<p_0\approx 2084$ bars the volume fraction of the low-density component is high. When T increases, the increasing role of entropy leads first to mixing of the locally ordered and disordered components that occurs at a relatively low energy cost. Hence, density increases. Further heating leads to a still more important role of entropy. As a consequence, the two components start to mix with empty cells —this occurs at a larger energy cost than mixing of the locally ordered and locally disordered components. The presence of the empty cells leads in turn to a decrease of density, as shown schematically in Fig. 10.

The EOS, thermal expansion, isobaric heat capacity, correlation length, and compressibility also show qualitative

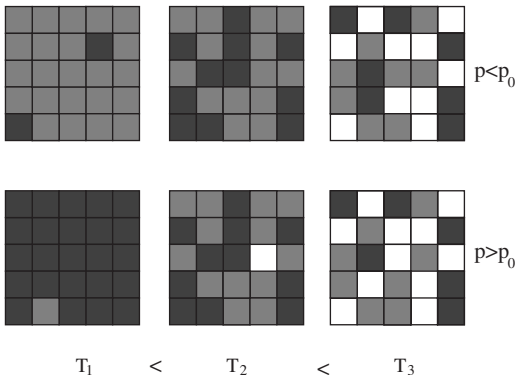

FIG. 10. Schematic showing a sequence of typical configurations for $p<p_0\approx 2000$ bars (top) and $p>p_0\approx 2000$ bars (bottom) and three different temperatures. Density ratio between the dark gray and light-gray regions is $1+2\delta>1$. For more explanations concerning the symbolic representation of the mesoscopic states, see Fig. 1.

features characteristic of water, but pressure is significantly overestimated in the simple MF approximation. Overestimated pressure is expected for the lattice models and in the MF approximation, and this deficiency will be removed (to some extent at least) in the off-lattice version of the model that we plan to develop. Beyond the MF approximation pressure should be lower; the effect of fluctuations depends on T, and the slope of the coexistence lines can be significantly different in an exact solution of our model.

Orientational ordering of water molecules is not taken into account directly, but only through the existence of the locally ordered water, which results from the orientational ordering. Orientational degrees of freedom certainly influence quantitative results for the grand potential (pressure) and entropy; for quantitative agreement of the EOS with real water, the generic model is certainly oversimplified. On the qualitative level the only result that disagrees with common expectations is the slope of the (metastable) liquid-liquid coexistence line $p(T)$, which is positive (but very small) in the simple MF approximation. The slope of this line beyond the MF approximation is not known; it might be negative, but large negative values are not expected. This is a direct consequence of not taking into account the difference in entropy associated with *local* ordering in the cells occupied by the LDW and HDW states respectively.

We have shown that the model as simple as the BEG model with properly adjusted parameters is capable of predicting the distinctive anomalies of water. This result suggests that the entropy associated with different spatial distributions of the locally ordered and disordered regions is responsible for all the water anomalies, since they are found even when the entropy associated with *local* ordering in the locally ordered and locally disordered structures is disregarded.

Finally, the relative success of this simple model in the simplest MF approximation indicates that similar approach can be used to study other associating liquids, such as alcohols, for example, as well as aqueous mixtures with polar molecules.

ACKNOWLEDGMENTS

This work was partially supported by the Polish Ministry of Science and Higher Education, Grant No. NN 202 006034 and partially by the POLONIUM project.

APPENDIX A: SPINODAL LINE

The explicit forms of (40) and (41) are the following:

$$\mu=\left[\frac{kT}{2}\ln\left(\frac{\eta+s}{\eta-s}\right)-6J^{ll}s-6Q\eta\right]\delta^{-1}, \tag{A1}$$

$$\mu=\left[\frac{kT}{2}\ln\left(\frac{\eta^2-s^2}{4(1-\eta)^2}\right)-24J^{gl}\eta-6Qs\right](1+\delta)^{-1}. \tag{A2}$$

From Eq. (42) we obtain the explicit expression for the spinodal surface in the (η,s,T) variables:

$$kT_s(\eta,s)=-b(\eta,s)+\sqrt{\Delta_s(\eta,s)}, \tag{A3}$$

where

$$\Delta_s(\eta,s)=b(\eta,s)^2-36(4J^{ll}J^{gl}-Q^2)(\eta^2-s^2)(1-\eta), \tag{A4}$$

$$b(\eta,s)=-3[J^{ll}\eta+4J^{gl}\eta(1-\eta)+2Qs(1-\eta)-J^{ll}s^2]. \tag{A5}$$

From the relation (43) we can obtain temperature as a function of η and s. By equating this temperature with T_s given in (A3), we find that along the spinodal line the relation between η and s is given by

$$-b(\eta,s)+\sqrt{\Delta_s(\eta,s)}=\frac{12\{[(1+\delta)J^{ll}-\delta Q]s+[(1+\delta)Q-4J^{gl}\delta]\eta\}}{\ln\left[\frac{\eta+s}{\eta-s}\left(\frac{2(1-\eta)}{\eta-s}\right)^{2\delta}\right]}. \tag{A6}$$

APPENDIX B: PHASE EQUILIBRIA

Equations (40) and (41) can be written in the form

$$s=F_s(s,\eta|,\mu,T),\quad \eta=F_\eta(s,\eta|,\mu,T), \tag{B1}$$

where

$$F_\eta(s,\eta|,\mu,T)=\frac{2\cosh(\beta R_s)e^{\beta R_\eta}}{\Xi_0}, \tag{B2}$$

$$F_s(s,\eta|,\mu,T)=\frac{2\sinh(\beta R_s)e^{\beta R_\eta}}{\Xi_0}, \tag{B3}$$

$$\Xi_0=2\cosh(\beta R_s)e^{\beta R_\eta}+1, \tag{B4}$$

$$R_s=6(J^{ll}s+Q\eta)+\delta\mu, \tag{B5}$$

$$R_\eta=6(4J^{gl}\eta+Qs)+(1+\delta)\mu. \tag{B6}$$

We look for the fixed points of (B1) by using iterations $(s_{i+1}=F_s(s_i,\eta_i),\eta_{i+1}=F_\eta(s_i,\eta_i))$. The solutions give s and η

in the stable or metastable phase for given T and μ. The stable phase corresponds to a lower value of $-pv_0$. At the phase equilibria, $pv_0(s^\alpha,\eta^\alpha)=pv_0(s^\beta,\eta^\beta)$, where α and β denote the two coexisting phases. This method allows also for obtaining the EOS isotherms $p(\bar{\rho})$.

APPENDIX C: EOS

Here we describe the method for obtaining the EOS isobars. From Eq. (48) we obtain $s=s_1(\eta,kT,p)$ or $s=s_2(\eta,kT,p)$, where

$$s_{1,2}(\eta,kT,p)=\frac{-6Q\eta\pm\sqrt{\Delta(\eta,kT,p)}}{6J^{ll}} \tag{C1}$$

and

$$\Delta(\eta,kT,p)=36Q^2\eta^2-12J^{ll}[p+12J^{gl}\eta^2+kT\ln(1-\eta)]. \tag{C2}$$

The EOS is given by the parametric equations

$$\bar{\rho}(\eta,kT,p)=(1+\delta)\eta+\delta s_1(\eta,kT,p) \tag{C3}$$

and

$$F_1(\eta,kT,p)=0 \tag{C4}$$

if Eq. (C4) has a solution. When Eq. (C4) has no solutions, the EOS is given by the parametric equations

$$\bar{\rho}(\eta,kT,p)=(1+\delta)\eta+\delta s_2(\eta,kT,p) \tag{C5}$$

and

$$F_2(\eta,kT,p)=0, \tag{C6}$$

where

$$F_i(\eta,kT,p)=kT\ln\left[\frac{\eta+s_i}{\eta-s_i}\left(\frac{2(1-\eta)}{\eta-s_i}\right)^{2\delta}\right]-12\{[(1+\delta)J^{ll}-\delta Q]s_i+[(1+\delta)Q-4J^{gl}\delta]\eta\}. \tag{C7}$$

The latter relation follows from (43). Depending on parameters, either (C4) or (C6) has solutions. Accordingly, the density is given either in Eq. (C3) or (C5), respectively.

APPENDIX D: CORRELATION FUNCTION

The explicit forms of the coefficients in Eq. (60) are the following:

$$A_{N0}=[(1+\delta)^2+\delta^2]\,(1-\eta)\eta+2\delta(1+\delta)](1-\eta)s+\delta^2(\eta^2-s^2), \tag{D1}$$

$$A_{N1}=[2\delta(1+\delta)Q-4\delta^2J^{gl}-(1+\delta)^2J^{ll}](1-\eta)(\eta^2-s^2)=-h(1+2\delta)^2, \tag{D2}$$

$$A_{D1}=-[4J^{gl}(1-\eta)\eta+J^{ll}(\eta-s^2)+2Qs(1-\eta)], \tag{D3}$$

$$A_{D2}=(4J^{gl}J^{ll}-Q^2)(1-\eta)(\eta^2-s^2). \tag{D4}$$

[1] W. K. Roentgen, Ann. Phys. **45**, 91 (1892).
[2] L. Pauling, in *Hydrogen Bonding*, edited by D. Hadzi and H. W. Thompson (Pergamon Press, London, 1959).
[3] H. S. Frank and W.-Y. Wen, Discuss. Faraday Soc. **24**, 133 (1957).
[4] G. W. Robinson, C. H. Cho, and J. Urquidi, J. Chem. Phys. **111**, 698 (1999).
[5] S. Woutersen, U. Emmerichs, and H. J. Bakker, Science **278**, 658 (1997).
[6] M. Sasai, Physica A **285**, 315 (2000).
[7] H. J. Bakker, Chem. Rev. (Washington, D.C.) **108**, 1456 (2008).
[8] F. Franks, *Water: A Comprehensive Treatise* (Plenum Press, London, 1973), Vol. 3.
[9] B. Widom, P. Bhimalapuram, and K. Koga, Phys. Chem. Chem. Phys. **5**, 3085 (2003).
[10] A. Pertsemlidis, A. M. Saxena, A. K. Soper, T. Head-Gordon, and R. M. Glaeser, Proc. Natl. Acad. Sci. U.S.A. **93**, 10769 (1996).
[11] G. W. Robinson, C. H. Cho, and J. Urquidi, J. Chem. Phys. **111**, 698 (1999).
[12] H. Poole, F. Sciortino, U. Essmann, and H. E. Stanley, Nature (London) **360**, 324 (1992).
[13] S. S. Borick, P. G. Debenedetti, and S. Sastry, J. Phys. Chem. **99**, 3781 (1995).
[14] H. E. Stanley, L. Cruz, S. T. Harrington, P. H. Poole, S. Satstry, F. Sciortino, F. W. Starr, and R. Zhang, Physica A **236**, 19 (1997).
[15] I. Brovchenko, A. Geiger, and A. Oleinikova, J. Chem. Phys. **123**, 044515 (2005).
[16] J. Roberts and P. G. Debenedetti, J. Chem. Phys. **105**, 658 (1996).
[17] S. Sastry, P. G. Debenedetti, F. Sciortino, and H. E. Stanley, Phys. Rev. E **53**, 6144 (1996).
[18] P. H. Poole, F. Sciortino, T. Grande, H. E. Stanley, and C. A. Angell, Phys. Rev. Lett. **73**, 1632 (1994).
[19] A. Angell, Science **319**, 582 (2008).
[20] For an interesting comparison of different scenarios, see K. Stoney, M. G. Mazza, H. E. Stanley, e-print arXiv:cond-mat/0805.3468.
[21] G. M. Bell, J. Phys. C **5**, 889 (1972).
[22] Z. Yan, S. V. Buldyrev, N. Giovambattista, P. G. Debenedetti, and H. E. Stanley, Phys. Rev. E **73**, 051204 (2006).
[23] A. Barros de Oliveira, G. Franceze, P. A. Netz, and M. C. Barbosa, J. Chem. Phys. **128**, 064901 (2008).
[24] E. Lomba, N. G. Almarza, C. Martin, and C. McBride, J. Chem. Phys. **126**, 244510 (2007).
[25] P. C. Hemmer and G. Stell, Phys. Rev. Lett. **24**, 1284 (1970).
[26] H. Tanaka, Phys. Rev. Lett. **80**, 5750 (1998).
[27] H. S. Ashbaugh, T. M. Truskett, and P. G. Debenedetti, J.

Chem. Phys. **116**, 2907 (2002).
[28] S. Chatterjee, H. S. Ashbaugh, and P. G. Debenedetti, J. Chem. Phys. **123**, 164503 (2005).
[29] T. M. Truskett, P. G. Debenedetti, S. Torquato, and S. Sastry, J. Chem. Phys. **111**, 2647 (1999).
[30] L. Zoranic, R. Mazighi, F. Sokolic, and A. Perera, J. Phys. Chem. **111**, 15586 (2007).
[31] G. Gompper and M. Schick, *Self-Assembling Amphiphilic Systems*, 1st ed., Vol. 16 of *Phase Transitions and Critical Phenomena* (Academic Press, San Diego, 1994).
[32] A. Ciach, J. Høye, and G. Stell, J. Phys. A **21**, L777 (1988).
[33] A. Ciach and J. Høye, J. Chem. Phys. **90**, 1222 (1989).
[34] A. Ciach, J. Chem. Phys. **96**, 1399 (1992).
[35] A. Ciach and W. T. Góźdź, Annu. Rep. Prog. Chem., Sect. C: Phys. Chem. **97**, 269 (2001).
[36] M. Blume, V. J. Emery, and R. B. Griffith, Phys. Rev. A **4**, 1071 (1971).